Spin distribution in plastically deformed Fe - Al intermetallic compounds

1996 J. Phys.: Condens. Matter 8 11243

(http://iopscience.iop.org/0953-8984/8/50/045)

J. Phys.: Condens. Matter **8** (1996) 11243–11257. Printed in the UK

Spin distribution in plastically deformed Fe–Al intermetallic compounds

S Takahashi, X G Li and A Chiba

Faculty of Engineering, Iwate University, Morioka 020, Japan

Received 16 July 1996, in final form 23 September 1996

Abstract. The influence of plastic deformation on the magnetic properties has been studied in Fe–Al intermetallic compounds with composition between 30 and 40 at.% Al. The spontaneous magnetization, M_s, increases considerably as a result of plastic deformation between 30 and 34 at.% Al concentration. The Fe–Al compounds containing between 35.0 and 50.0 at.% Al are paramagnetic before plastic deformation and as a result of plastic deformation the magnetic susceptibility increases remarkably. At the same time M_s appears. The ferromagnetic clusters are induced by plastic deformation along the antiphase boundary (APB) ribbons between superpartial dislocations. The cluster along the APB ribbon shows a strong anisotropy whose easy direction of magnetization is ⟨100⟩ within the {110} glide plane. The easy direction of magnetization is consistent with that of the roll-induced anisotropy in Fe_3Al alloys. The origin of the spin glass in these compounds is explained by the magnetic anisotropy depending on the atomic arrangement. The conditions of the transition to the ferromagnetic state are discussed.

1. Introduction

FeAl intermetallic compounds have three magnetic states, paramagnetic, ferromagnetic and spin-glass states. The spin-glass state is observed at low temperatures between 27 and 50 at.% Al, containing frozen moments of all orientations but without long-range order of either ferromagnetic or antiferromagnetic type. The spin-glass state in this compound is explained generally by the competition between ferromagnetic and antiferromagnetic interactions, so called, 'frustration'. There exist two exchange interactions between all moments, with positive and negative exchange parameters, and there is no reasonable arrangement that satisfies all the microscopic constraints.

A microscopic model was introduced by Shukla and Wortis (1980) to explain the spin-glass behaviour in Fe–Al compounds. Fe–Al intermetallic compounds have the B2-type ordered structure; Fe atoms occupy the corner sites in the body centred cubic structure (the α-site), and Al atoms and the rest of the Fe atoms occupy randomly the centre site (the β-site). There are two atomic configurations in the B2-type Fe–Al intermetallic compounds and the exchange interaction is different in these atomic configurations (Arrott and Sato 1959, Sato and Arrott 1959). When an Al atom occupies the β-site site there is an indirect antiferromagnetic interaction between each of 12 Fe–Fe cube-edge pairs. When the β-site is occupied by an Fe atom, there is a ferromagnetic interaction between the β-site Fe atom and its eight nearest neighbours (NNs). The spin glass is explained by these two atomic configurations in the compounds. According to this model, the stoichiometric Fe–Al compound would be antiferromagnetic at sufficiently low temperature, but this result contradicts experiment (Parthasarathi and Beck 1976). The neighbouring effect has been

0953-8984/96/5011243+15$19.50

added to the model to solve the contradiction. The size of magnetic moment depends on the number of the NN Fe atoms, and it disappears when the number of the first-NN Fe atoms is less than three. There are no first NN Fe atoms in the stoichiometric Fe–Al compound.

Our interest in these compounds is the magnetic transition due to plastic deformation. Fe–Al compounds with more than 35.0 at.% Al concentration are paramagnetic before plastic deformation. After plastic deformation the magnetic susceptibility increases remarkably and at the same time the spontaneous magnetization, M_s appears. The magnetic transition is observed even near and at the stoichiometric composition (Taylor and Jones 1958).

The magnetic transition due to plastic deformation was explained in terms of the number of first- and second-NN Fe atoms (Huffman and Fisher 1967, Besnus *et al* 1975) and from the viewpoint of the atomic arrangement in the vicinity of the antiphase boundary (APB) (Huffman and Fisher 1967). The value of M_s has been expressed by a simple function of dislocation density by one of the present authors (Takahashi 1986).

Ferromagnetic clusters are present along the APB ribbons between superpartial dislocations. The number of Fe atoms around the host α- and β-site Fe atoms in the vicinity of the APB is nearly the same or the same as in the ordered state within the first- or/and the second-NN cell. Thus the appearance of M_s cannot be interpreted only in terms the number of NN Fe atoms (Takahashi and Umakoshi 1990, 1991). In the vicinity of the APB, the α-site Fe atoms are arranged in a chain with their first NNs. The geometric arrangement of Fe atoms plays an important role in the magnetic transition rather than the number of the NN Fe atoms. This conclusion contradicts the model proposed by Shukla and Wortis (1980). One purpose of the present study is to investigate the spin-glass behaviour in Fe–Al compounds and the influence of plastic deformation on the spin-glass state.

Another magnetic phenomenon due to plastic deformation is the roll-induced magnetic anisotropy (Chikazumi *et al* 1960). A strong uniaxial magnetic anisotropy was found to be induced by cold rolling in Fe_3Al alloys. The roll-induced anisotropy was explained in terms of the atomic configuration in the vicinity of the APB between superpartial dislocations (Takahashi 1972, 1975). It is also proposed for the roll-induced anisotropy in the Fe_3Al alloy that the direction of easy magnetization depends on the order structures and the glide plane; the direction of easy magnetization in the DO_3- type superlattice is that of hard magnetization in the B2-type superlattice, when the same slip system works. Another purpose of this study is to investigate the magnetic anisotropy of the ferromagnetic clusters along the APB ribbons in Fe–Al compounds. Furthermore, the relationship between the two types of magnetic anisotropy will be discussed.

The transition from paramagnetism to ferromagnetism has been explained by the number of NN Fe atoms (Huffman and Fisher 1967, Besnus *et al* 1975). Their explanation cannot be applied to the ferromagnetic state of the APB ribbons and another rule is necessary for the ferromagnetic APB ribbons induced by plastic deformation. The condition for ferromagnetism in Fe–Al compounds will be discussed on the basis of the experimental results.

2. Experimental procedure

The raw materials used for alloying were 99.998 mass% Al and 99.95 mass% Fe. Alloy 'buttons' with the nominal composition of 30.0, 31.0, 35.0, 36.0, 37.0, 39.0, and 40.0 at.% Al–Fe were prepared by arc melting the raw materials four times to attain chemical homogeneity on a water-cooled copper hearth in an argon gas atmosphere at a pressure of approximately 93 kPa. As weight losses after the arc melting were smaller than 0.1% for an ingot, the nominal composition was regarded as the chemical composition. The buttons

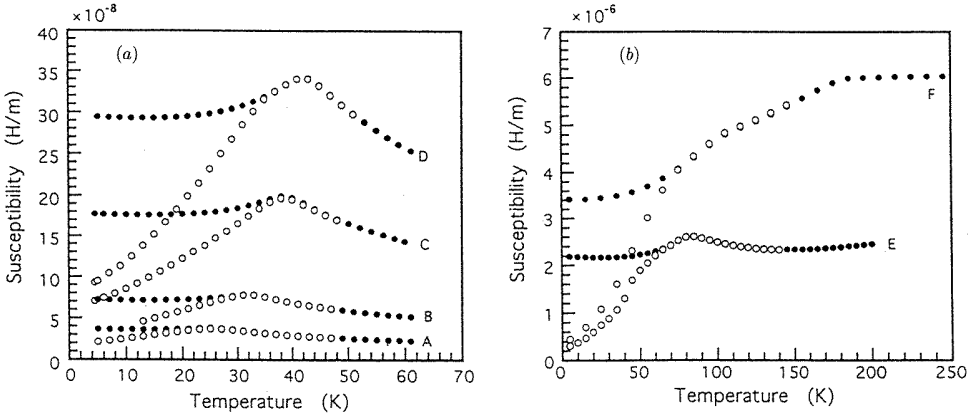

Figure 1. Magnetic susceptibility versus temperature for 40 at.% (A), 37 at.% (B), 36 at.% (C), 35 at.% (D), 31 at.% (E), and 30 at.% (F) Al–Fe intermetallic compounds. Samples were cooled to 4.5 K under zero field, measurements were made in a sequence of increasing temperatures (open circles), and samples were cooled and measured under 50 Oe (solid circles).

were homogenized at 973 K for 2 d. The samples, with dimensions of approximately $2.5 \times 2.5 \times 5.0$ mm^3 were cut from the button ingot and chemically polished to remove surface damage. The mean grain size was 0.1–0.3 mm in each sample. The samples were tested in compression at room temperature by an Instron-type machine. Samples for the magnetic measurement, with dimensions of $2.5 \times 2.5 \times 2.5$ mm^3, were formed by a Servomet spark machine. Surface damage of the sample was removed by chemical polishing. The steady-field magnetization was measured by a SQUID magnetic fluxmeter (Quantum Design) in the temperature range from 4.5 to 300 K. Thin foils for electron microscopy investigation were prepared from the rectangular prisms by spark machining and finally thinned using a standard jet-electropolishing technique. Superlattice dislocations were observed in the foil on a 200 kV transmission electron microscope.

3. Experimental results

3.1. Magnetic measurements

Figure 1(*a*) and (*b*) shows the temperature dependence of the magnetic susceptibility (with a magnetization of 50 Oe) for 35, 36, 37, and 40 at.% Al–Fe compounds and 30 and 31 at.% Al–Fe compounds, respectively, without plastic deformation. The thermomagnetic curves were recorded by two different procedures: first cooled to 4.5 K in zero field, then measured in a sequence of increasing temperatures (open circles), and samples were cooled and measured in a field of 50 Oe (solid circles). These steady-field magnetization curves show clearly the thermomagnetic hysteresis effect typical for a spin glass (Shull *et al* 1976). The cusp in the thermomagnetization curve corresponds to the freezing temperature, T_f, according to the previous investigators (Okamoto and Beck 1971, Shull *et al* 1976). The shape of the cusp is sharp in the 35 at.% Al–Fe and becomes indistinct with increasing and decreasing Al content. The temperature of the cusp increases with decreasing Al content.

Figure 2 shows T_f versus Al content, in comparison to the results of the previous work (Shull *et al* 1976). The latter authors obtained T_f from the relation of alternating low-field

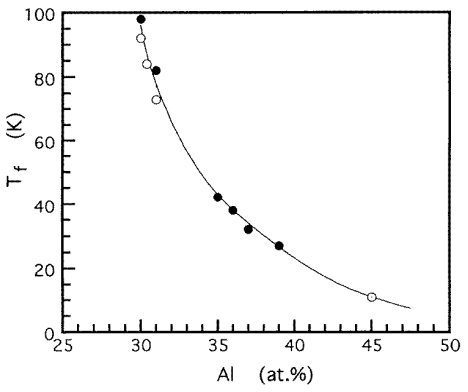

Figure 2. Freezing temperature, T_f, versus Al content in Fe–Al compounds, comparing the present results (solid circles) with those of the previous study (Shull *et al* 1976) (open circles).

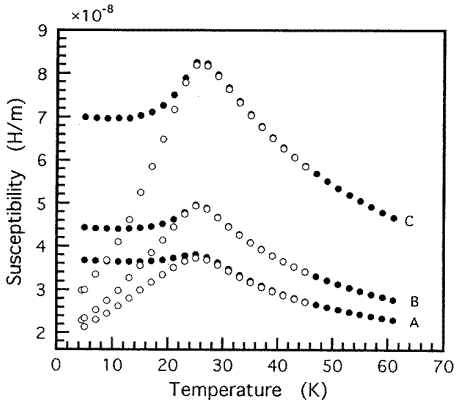

Figure 3. Magnetic susceptibility versus temperature for the 40 at.% Al–Fe intermetallic compound without plastic deformation (A) and with plastic deformation of 5% (B) and 10% (C). Samples were cooled to 4.5 K under zero field, measurements were made in a sequence of increasing temperatures (open circles), and samples were cooled and measured under 50 Oe (solid circles).

susceptibility versus temperature. The present result (solid circles) is consistent with the previous one (open circles). The temperature of the cusp may be defined as the freezing temperature of the spin glass.

Figure 3 shows the magnetic susceptibility versus temperature for the 40 at.% Al–Fe compound without plastic deformation and with plastic deformation of $\varepsilon = 5$ and 10%. Plastic deformation increases the magnetic susceptibility and the cusp becomes sharp. T_f increases slightly with increasing plastic strain. Figure 4 shows the thermomagnetic curves of the 36 at.% Al–Fe compound before and after plastic deformation. The same tendency in the behaviour of the magnetic susceptibility can be observed as for the 40 at.% Al–Fe compound. The increase of T_f due to plastic deformation is found in other Fe–Al compounds with 30, 31, 35, and 39 at.% Al contents. The plastic strain dependence of T_f is shown in figure 5. T_f increases with increasing strain and the increase of T_f as a result of plastic strain becomes more pronounced with decreasing Al content; T_f increases from 25.5 to 26.2 K as a result of 10% strain in the 40 at.% Al–Fe compound and in the 36 at.% Al–Fe compound T_f increases from 38.5 to 46.2 K with 10% strain.

In 30 and 31 at.% Al–Fe compounds, the same dependence of T_f on strain is obtained, but two remarkable features have been found in these compounds with plastic deformation. A strong uniaxial anisotropy appears in the thermomagnetic curves. Figure 6(a), (b) and (c) shows the thermomagnetic curves in the 31 at.% Al–Fe compound with plastic deformation of $\varepsilon = 5$, 7 and 9%, respectively. In each part, the thermomagnetic curves were measured on applying the external magnetic field in two directions, parallel and perpendicular to the compression axis. The magnetic susceptibility with the magnetic field applied perpendicular to the compression axis is larger than that with it parallel to the axis. The difference of the thermomagnetic curves appears when the measurement is performed cooling the sample in the magnetic field. The anisotropy in the thermomagnetic curve is also observed in the 30 at.% Al–Fe compound. An unexpected result is obtained in the thermomagnetic curves in the 31 at.% Al–Fe compound with plastic deformation of $\varepsilon = 5$, 7, and 9%. The magnetic

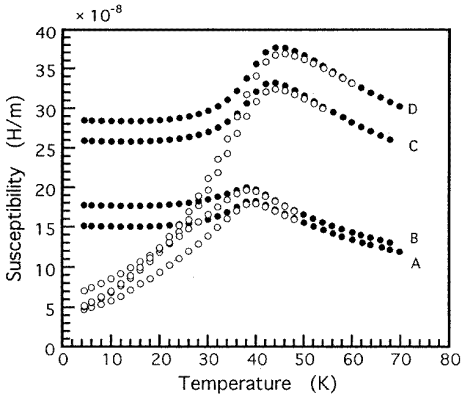

Figure 4. Magnetic susceptibility versus temperature for the 36 at.% Al–Fe intemetallic compound without plastic deformation (A) and with plastic deformation of 5% (B), 8% (C), and 10% (D). Samples were cooled to 4.5 K under zero field, measurements were made in a sequence of increasing temperatures (open circles), and samples were cooled and measured under 50 Oe (solid circles).

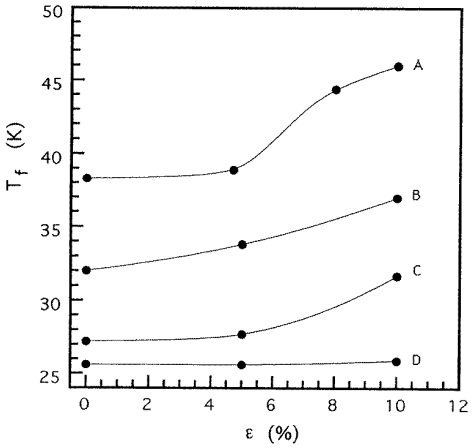

Figure 5. Freezing temperature, T_f, versus plastic strain, ε in 36 at.% (A), 37 at.% (B), 39 at.% (C), and 40 at.% (D) Al–Fe compounds.

susceptibility increases with plastic strain of $\varepsilon = 5\%$, it decreases with higher strain. This tendency is different from that of the 36 and 40 at.% Al–Fe compounds (see figures 3 and 4).

The magnetization measurement is made in the 30 at.% Al–Fe compound to estimate the strength of the magnetic anisotropy. Figures 7 and 8 show the magnetization curves on applying the magnetic field parallel and perpendicular to the compression axis in the plastic deformation of $\varepsilon = 8.6$ and 12%, respectively. The magnetization was measured at 150 K where the ferromagnetic state due to plastic deformation coexists with the paramagnetic state. The magnetization with the magnetic field applied perpendicular to the compression axis is larger than that with it parallel. The direction of easy magnetization is present near the direction perpendicular to the compression axis. The two magnetization curves do not meet at 0.5 MA m^{-1}. In an iron single crystal, for example, the magnetization curve in the direction of hard magnetization meets with that of easy magnetization at 5×10^{-2} MA m^{-1}. The magnetization curves in the two directions meet at 2 MA m^{-1} as shown in figure 9.

3.2. The observation of superlattice dislocations

The dislocation structure has been observed with an electron microscope. Figure 10 shows the electron micrograph of the 30 at.% Al–Fe compound after plastic deformation of $\varepsilon = 5\%$. The electron microscopy observation indicates that paired dislocations are distributed on {110} glide planes. The separation of partial dislocations is determined according to the previous observation of the weak-beam image superlattice dislocations by one of the present authors and his coworker (Takahashi and Umakoshi 1990); a superlattice dislocation is dissociated into two superpartials and the separation of partial dislocations is 28–35 nm in a 40 at.% Al content alloy. The value of dislocation density, ρ, was measured by counting the

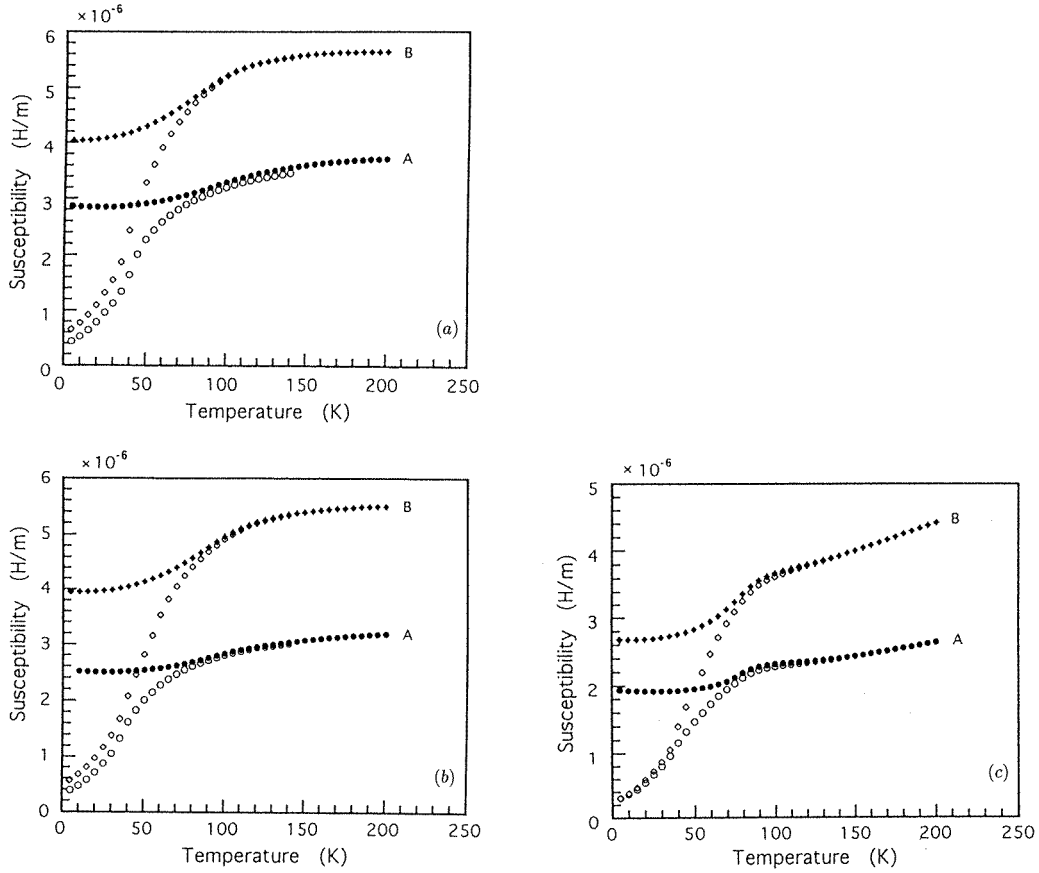

Figure 6. Magnetic susceptibility versus temperature for the 31 at.% Al–Fe intermetallic compound with plastic deformation of (*a*) 5%, (*b*) 7%, and (*c*) 9%. Measurements were made on applying magnetic field parallel (A) and perpendicular (B) to the compression axis. Each sample was cooled to 4.5 K under zero field, measurements were made in a sequence of increasing temperatures (open symbols), and samples were cooled and measured under 50 Oe (solid symbols).

intersection of dislocation lines with straight lines drawn randomly on photographic films. The thickness of the foil is estimated to be 80–120 nm by counting the number of thickness fringes from the edge of the specimen. The observed dislocation density may include about 30% error which arises from the uncertainty of foil thickness. ρ is approximately 8×10^9 cm^{-2} in the sample with $\varepsilon = 5\%$. These superlattice dislocations have APBs between superpartials.

Figures 11 and 12 are the electron micrographs of the 30 at.% Al–Fe compound deformed plastically by $\varepsilon = 9$ and 11%, respectively. The superpartials make a pair. $\rho = 1.3 \times 10^{10}$ cm^{-2} at $\varepsilon = 9\%$ and $\rho = 3 \times 10^{10}$ cm^{-2} at $\varepsilon = 11\%$.

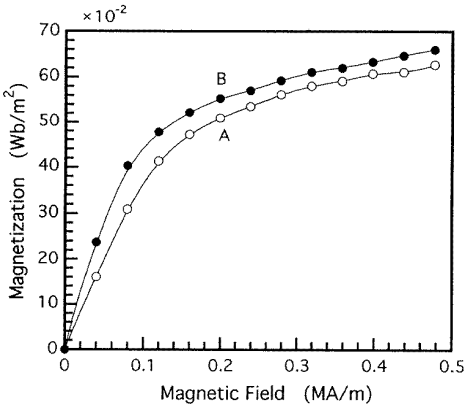

Figure 7. Magnetization curves of the 30 at.% Al–Fe compound with plastic deformation of 8.6% strain. Measurements were made at 150 K on applying a magnetic field parallel (A) and perpendicular (B) to the compression axis.

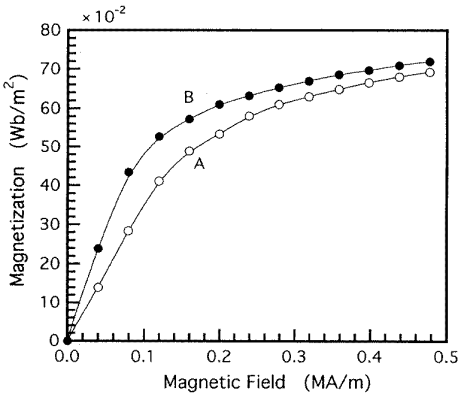

Figure 8. Magnetization curves of the 30 at.% Al–Fe compound with plastic deformation of 12% strain. Measurements were made at 150 K on applying a magnetic field parallel (A) and perpendicular (B) to the compression axis.

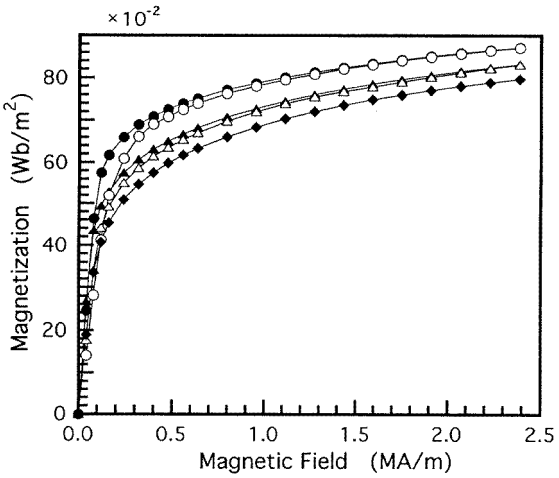

Figure 9. Magnetization curves of the 30 at.% Al–Fe compound without plastic deformation (♦) with plastic deformation of 5% (△, ▲) and 12% (○ , ●) strain. Measurements were made at 200 K on applying magnetic field parallel (△, ○) and perpendicular (▲, ●) to the compression axis.

4. Atomic arrangement near APB

4.1. Magnetic transition due to plastic deformation

In the B2-type structure of Fe–Al intermetallic compounds, superlattice dislocations are induced by plastic deformation and play an important role in the magnetic transition due to plastic deformation. The leading superpartial dislocation creates an APB on the {110} glide plane after it has slipped. In the vicinity of the APB, the arrangement of Fe and Al atoms is different from that in the ordered state.

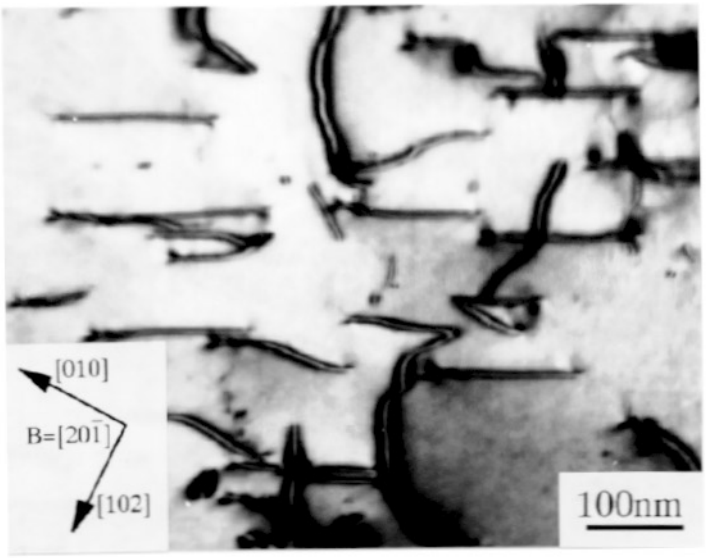

Figure 10. An electron micrograph of the 30 at.% Al–Fe intermetallic compound with 5% strain. *B* indicates the electron beam direction.

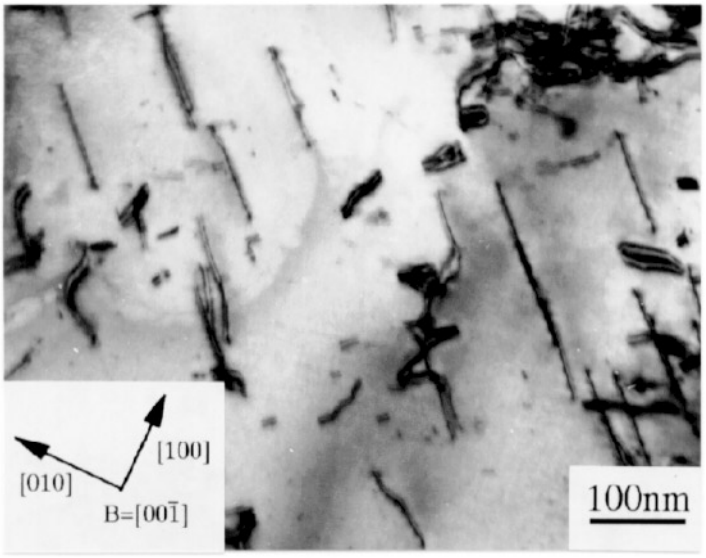

Figure 11. An electron micrograph of the 30 at.% Al–Fe intermetallic compound with 9% strain. *B* indicates the electron beam direction.

Plastic deformation causes the magnetic transition from paramagnetic to ferromagnetic in Fe–Al intermetallic compounds. The coexistence of paramagnetic and ferromagnetic states or that of two ferromagnetic structures is observed in the plastically deformed compounds. Considering the crystal structure before and after plastic deformation, no change is admitted in the crystal but for the introduction of superlattice dislocations with APB. The cause of the magnetic transition due to plastic deformation must be the atomic arrangement in the

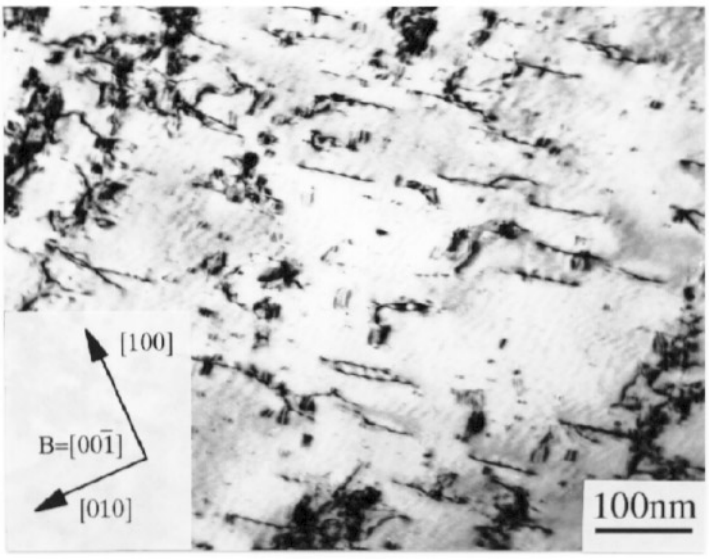

Figure 12. An electron micrograph of the 30 at.% Al–Fe intermetallic compound with 11% strain. B indicates the electron beam direction.

vicinity of the APB. Figure 13 shows the schematic arrangement of the α-site Fe atoms in the vicinity of the APB along the (011) glide plane. In the vicinity of the APB, the α-site Fe atoms are arranged in a chain with their first-NNs in the [100] direction. It is reasonable to conclude that the α-site Fe atoms arranged in a chain with their first-NNs in the [100] direction behave ferromagnetically. The number of chained Fe atoms in $Fe_{(1+c)}Al_{(1-c)}$ compounds is given by

$$N'_\alpha = \left\{r_0/\left(2^{1/2}a^2\right)\right\}\rho \tag{1}$$

and the number of β-site Fe atoms in the vicinity of the APB is given by

$$N'_\beta = \left\{\left(cr_0\right)/\left(2^{1/2}a^2\right)\right\}\rho \tag{2}$$

where a is the lattice constant and r_0 (=35 nm) is the separation of superpartial dislocations or the width of an APB ribbon (Takahashi 1986).

If the effects of the magnetic transition from paramagnetism to ferromagnetism are extended as far as the nth-NN distance from the APB, the number of ferromagnetically coupled Fe atoms is $N_i = nN'_i$. The net spontaneous magnetization of the plastically deformed Fe–Al alloys at 0 K is given as

$$M_s(0) = M_0 + N_\alpha\left(\mu'_\alpha - \mu_\alpha\right) + N_\beta\left(\mu'_\beta - \mu_\beta\right). \tag{3}$$

Here μ_α and μ_β are the magnetic moment of the α- and β-site Fe atoms in the ordered state, respectively, and μ'_α and μ'_β are those in the vicinity of the APB. M_0 is the spontaneous magnetization before plastic deformation.

4.2. Dipole–dipole interaction in roll-induced magnetic anisotropy

A strong uniaxial magnetic anisotropy is induced by plastic deformation besides the magneto-crystalline anisotropy in Fe_3Al atomically ordered alloys. This is known as roll-induced magnetic anisotropy. The roll-induced anisotropy is explained in terms of the

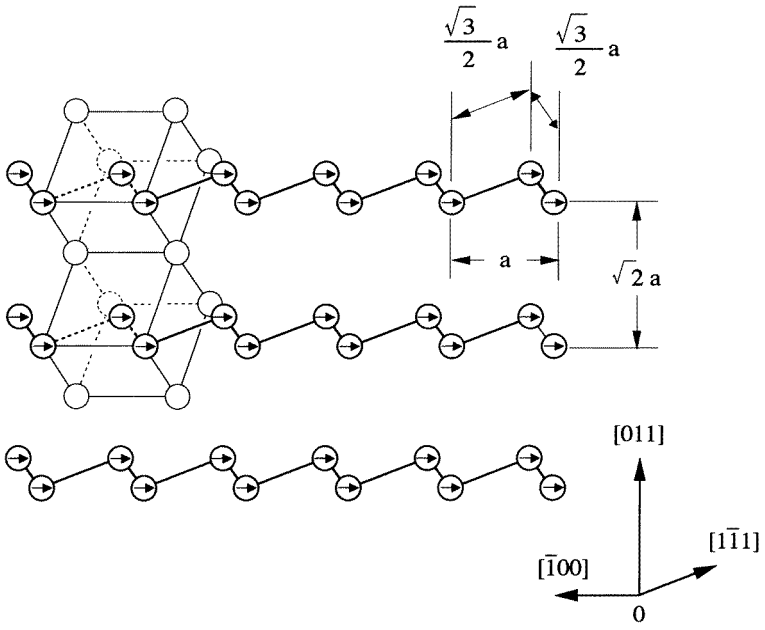

Figure 13. The schematic arrangement of the α-site Fe atoms along the $(0\bar{1}1)$ APB in the B2-type structure. Fe atoms chain at the first-NNs and are in a row in the [100] direction. The magnetic moment on the Fe atoms couples ferromagnetically and is directed along [100]. The arrows in the circles indicate the direction of easy magnetization.

dipole–dipole interaction (Néel 1954, Taniguchi and Yamamoto 1954, Chikazumi *et al* 1960). The induced anisotropy was considered from the viewpoint of the dislocation theory by one of the present authors (Takahashi 1972, 1975), and the direction of easy magnetization depends on the type of superlattice and glide planes. The roll-induced anisotropy is also caused by the atomic arrangement in the APB ribbon between superpartials. The uniaxial magnetic anisotropy in the APB ribbon between superpartials was confirmed by the observation of the domain structure by use of the electron microscope (Lapworth *et al* 1971, Jakubovics *et al* 1978). It seems reasonable to consider that the origin of the magnetic anisotropy in 30 and 31 at.% Al–Fe compounds with plastic deformation is the same as that of the roll-induced anisotropy in Fe_3Al atomically ordered alloys. The roll-induced magnetic anisotropy is written as

$$E = l_0 \sum N_{Al-Ali} \cos^2 \varphi_i = l_0 \sum N_{Fe-Fei} \cos^2 \varphi_i \tag{4}$$

where

$$l_0 = l_{Fe-Fe} + l_{Al-Al} - 2l_{Fe-Al}. \tag{5}$$

Here N_{B-Bi} is the number of B–B atom pairs directed in the ith pair direction, φ_i the angle between the magnetization and the ith pair direction, and l_{Fe-Fe}, l_{Al-Al}, and l_{Fe-Al} are the coefficients of dipole–dipole interaction of Fe–Fe, Al–Al, and Fe–Al, respectively. As the first-NN pairs do not contribute to the induced anisotropy in Fe–Al alloys (Chikazumi *et al* 1960), the number of second-NN atom pairs should be taken into consideration. l_0 of the second-NN pair is -4×10^{-14} erg in Fe_3Al atomically ordered alloys. When the

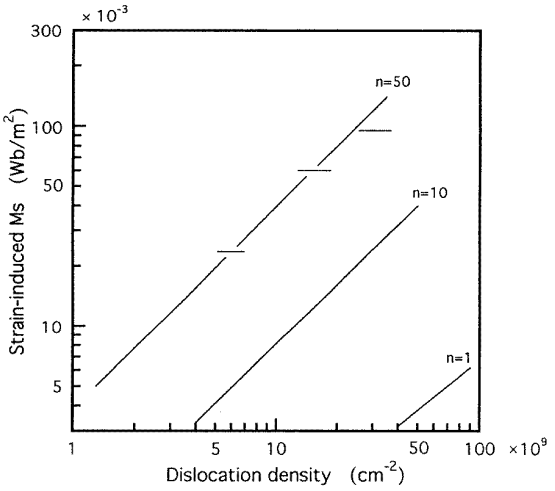

Figure 14. The relation between the strain-induced M_s and dislocation density ρ in comparison with the experimental results (segments of a line) for 30 at.% Al–Fe compound. The full lines are the calculated results. The experimental value of the induced M_s is that of 4.5 K and ρ is obtained by electron microscopic observation. n represents the degree of magnetic enhancement.

operating glide planes are (011) and $(0\bar{1}1)$ for example, the easy magnetization of the B2-type superlattice is in the [100] direction. The anisotropy is very strong: 10^4 times as strong as the magneto-crystalline anisotropy (Chikazumi *et al* 1960, Takahashi 1972).

5. Discussion

5.1. The ferromagnetic APB ribbon

In a previous paper by one of the authors and his coworker (Takahashi and Umakoshi 1991) the relation between M_s and ρ in (3) was compared with the experimental results, where the value at 77 K was used as $M_s(0)$. In the present study, M_s is measured at 4.5 K, and the relation is verified experimentally. Figure 14 shows the relation between the strain-induced M_s and ρ in comparison with the experimental results for 30 at.% Al–Fe compounds. The mean value of magnetic moments at the α- and β-sites is 0.5 μ_B, which is obtained from the experimental value of $M_0 = 32.1 \times 10^{-2}$ Wb m^{-2}, and the value in the vicinity of the APB is 2.2 μ_B. The experimental value of M_s is 50 times the calculated one: $n = 50$. The chained ferromagnetic Fe atoms enhance the neighbouring Fe atoms magnetically and change them to ferromagnetic as far as 50th-NNs. Actually the magnetic influence would extend further than $n = 50$, since the magnetic moment of the enhanced Fe atoms would be smaller than 2.2 μ_B. The value of n increases with increasing Fe content; $n = 2$–3 for 37 and 40 at.% Al contents and $n = 30$–40 for 34 at.% Al content (Takahashi and Umakoshi 1991). We shall discuss later the dependence of n on Fe content.

The relation of M_s and ρ in figure 14 shows that the ferromagnetic clusters along the APB ribbons are not transferred to the spin-glass state even at 4.5 K. There exist two magnetic states below T_f in the plastically deformed Fe–Al compounds. The same conclusion can be drawn from the experimental results shown in figures 3–6. The magnetic susceptibility of plastically deformed samples is very large compared to that of the undeformed ones, though the volume of APB ribbons is less than 10^{-3}% of the total volume

in the sample with $\varepsilon = 5\%$. The magnetic susceptibility in the spin-glass state increases considerably on introduction of the APB ribbons. The susceptibility in the APB ribbons would be 10^5 times as large as that of the B2-type ordered state. The large susceptibility in the plastically deformed samples suggests that the ferromagnetic state remains along the APB ribbons even in the temperature range between 4.5 K and T_f.

5.2. The magnetic anisotropy of the APB ribbons

A strong uniaxial anisotropy has been found in the plastically deformed 30 and 31 at.% Al–Fe compounds. The strong anisotropy is inherent in the ferromagnetic coupling of Fe atoms in the vicinity of APBs and the direction of easy magnetization depends on the atomic arrangement. The induced anisotropy in 30 and 31 at.% Al–Fe compounds is caused by the dipole–dipole interaction, as is the roll-induced anisotropy, since both phenomena are found in the same alloy system and caused by the introduction of the APBs between superpartial dislocations.

The samples are polycrystals with 0.1–0.3 mm grain size. When the sample is plastically deformed, small single crystals with a large Schmid factor contribute to the deformation. The probability would be large that the normal of the operating glide plane would be directed nearly $\pi/4$ to the compression axis. The Burgers vector of $(a/2)\ \langle 111\rangle$ should be within the glide plane and directed at nearly $\pi/4$ to the compression axis. The direction of easy magnetization is $\langle 100\rangle$ within $\{110\}$ glide plane according to (4), which is nearer to the direction perpendicular to the compression axis than that parallel to it. The conclusion on the direction of easy magnetization is consistent with the experimental results in 30 and 31 at.% Al–Fe compounds as shown in figures 6–8. The direction of magnetic moments localized at Fe atoms in the vicinity of the APB is shown in figure 13. The magnitude of the induced anisotropy is much stronger than that of the magneto-crystalline anisotropy and the direction of easy magnetization depends on the Fe and Al atomic arrangement. This rule would be adopted in the spin-glass state in B2-type Fe–Al intermetallic compounds without plastic deformation.

The strong magnetic anisotropy of the APB ferromagnetic cluster may explain the unexpected result of the strain dependence of magnetic susceptibility in 31 at.% Al–Fe compounds, as shown in figure 6. The ferromagnetic clusters enhance neighbouring Fe atoms and at the same time fix their magnetic moments firmly in the direction of easy magnetization. The sphere of influence is farther than 50 atomic distances from the APB ribbons. With the increase of plastic strain above 5%, the number of fixed moments increases and the number of magnetic moments which turn freely to the direction of the applied field decreases. On the other hand, in 36 and 40 at.% Al–Fe compounds the ferromagnetic clusters enhance the neighbouring Fe atoms, too, but the sphere of influence is small and strong anisotropy is not present in the ferromagnetic cluster. The magnetic susceptibility increases with plastic strain as shown in figures 3 and 4.

The direction of easy magnetization is $\langle 100\rangle$ within the glide plane, which is the same as that of the magneto-crystalline anisotropy in the B2-type structure, though the magneto-crystalline anisotropy cannot be explained by the magnetic dipole–dipole interaction. The magneto-crystalline anisotropy constant, K_1, in Fe_3Al atomically ordered alloys depends on the type of superstructure: in the DO_3-type superlattice it is -0.9×10^5 erg cm^3 and in the B2-type is 0.35×10^5 erg cm^3 (Takahashi 1975). The direction of easy magnetization in the DO_3-type superlattice is $\langle 111\rangle$ and that of the B2-type is $\langle 100\rangle$ in Fe_3Al atomically ordered alloys. In the intermetallic compounds used in the present study, the direction of easy magnetization is $\langle 100\rangle$ in the ferromagnetic state.

5.3. The origin of the spin glass and the conditions for ferromagnetism

The spin-glass state in Fe–Al intermetallic compounds is explained by the frustration in the coexistence of the ferromagnetic and antiferromagnetic structures. The complete antiferromagnetic structure can be expected in the stoichiometric composition at sufficiently low temperature, but the experimental result denies the expectation (Parthasarathi and Beck 1976). Another proposal was added by Shukla and Wortis (1980) to solve the discrepancy: the host Fe atom has no magnetic moment when the number of neighbouring Fe atoms is less than three. They explained the paramagnetic state near stoichiometry. We can observe the magnetic transition from paramagnetic to ferromagnetic due to plastic deformation even in the stoichiometric composition, though the number of neighbouring Fe atoms around the host α-site Fe atom is two in the vicinity of the APB (Takahashi and Umakoshi 1991). The coexistence of ferromagnetic and antiferromagnetic states is doubtful in Fe–Al intermetallic compounds. The presence of the antiferromagnetic state is not observed in the 30 at.% Al–Fe compound by the neutron-scattering method (Cable *et al* 1977). Another model is required to explain the frustration of the spin glass in Fe–Al intermetallic compounds.

In the ferromagnetic state of Fe–Al intermetallic compounds, there exists a magnetic anisotropy with the $\langle 100 \rangle$ direction of easy magnetization, but the direction of magnetic moments is restricted by the configuration of Fe and Al atoms and one of the $\langle 100 \rangle$ directions is selected by Fe–Fe atom pairs in the second-NNs. The existence of small ferromagnetic domains with different directions of easy magnetization would be possible. The neutron-scattering data show the presence of large ferromagnetic clusters in 30 at.% Al–Fe compounds (Cable *et al* 1977). The coexistence of small ferromagnetic domains produces the spin-glass state and the superparamagnetic state.

We discuss a concrete atomic configuration of the small ferromagnetic cluster. It seems appropriate to adopt the critical concentration of the transition from paramagnetism to ferromagnetism, i.e. 35 at.% Al. For simplicity, we consider a large lattice consisting of eight unit cells, where six Al atoms and two Fe atoms occupy randomly the β-site and all the α-sites are occupied by Fe atoms. The Al content is 37.5 at.%. One of the conditions for ferromagnetism in the B2-type structure is that in the large lattice, Fe atoms at the β-site align with second-NNs as shown in figure 15. The direction of easy magnetization is the pair direction of Fe atoms at the β-site according to the directional order model of (4), i.e. it is one of the $\langle 100 \rangle$ direction. This arrangement of Fe atoms, consisting of 12 α-site and two β-site Fe atoms, is the smallest unit for the ferromagnetic structure of Fe atoms as shown in figure 15. The second condition for ferromagnetism is the concentration of the smallest units, which depends on the critical distance of magnetic interaction between the smallest ferromagnetic units. The ferromagnetic cluster consists of the smallest ferromagnetic units with the same direction of easy magnetization. The density of ferromagnetic clusters increases with increasing Fe content and the ferromagnetic state changes from metastable to stable. The size of magnetic moment depends on the density of ferromagnetic clusters rather than the number of the NN Fe atoms. When the ferromagnetic clusters are introduced in the metastable ferromagnetic state by plastic deformation, the metastable state near the APB ribbon is enhanced and changes to the stable state. The degree of stability depends on the Fe content. The value of n, which depends also on the Fe content, determines the degree of stability as well as the growth of ferromagnetic clusters. The spin glass is caused by the competition of two ferromagnetic domains with different directions of easy magnetization.

The uniaxial and unidirectional anisotropy fields in the spin-glass state have been observed directly by NMR in the Cu–Mn alloy (Alloul 1979) and by simultaneous ESR

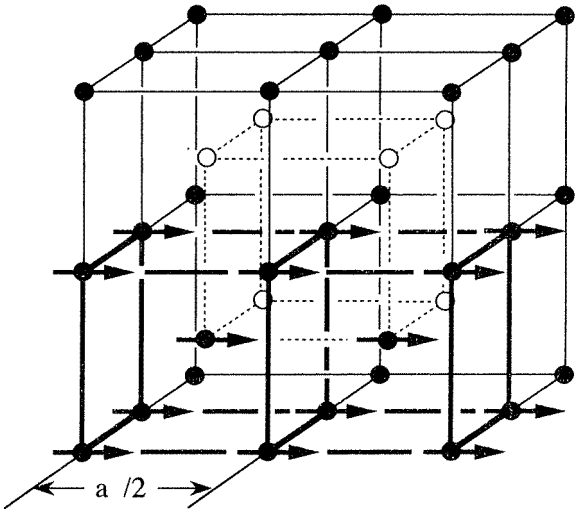

Figure 15. The atomic configuration of the smallest ferromagnetic unit in B2-type Fe–Al compounds. Two β-site Fe atoms form a pair at the second-NNs. The direction of easy magnetization is the pair direction of the β-site Fe atoms.

and magnetic measurements in Cu–Mn–Ni alloys (Shukla *et al* 1980). By cooling Fe–Al compounds in the magnetic field, unidirectional and uniaxial magnetic anisotropy are induced in the spin-glass state for 29–33 at.% Al concentration (Danan and Gengnagel 1968). The induced anisotropy is as strong as the roll-induced anisotropy, about 10^5 erg cm^3. The magnetic annealing effect would be caused by the rearrangement of Fe and Al atoms, so called directional order (Taniguchi and Yamamoto 1954). The existence of uniaxial anisotropy in Fe–Al compounds seems to be plausible and the origin of the spin glass would be the competition of small domains with different directions of easy magnetization.

The ferromagnetic state induced by plastic deformation remains even at 4.5 K, though the direct magnetic transition from ferromagnetic to spin glass can be observed just below 30 at.% Al composition. There exist two ferromagnetic states in the plastically deformed Fe–Al compounds, which are caused by different atomic configurations: one is produced by the B2-type superstructure and the other is the arrangement of the α-site Fe atoms in a chain with their first-NNs in the [001] direction. Since the large ferromagnetic cluster along the APB ribbon has a large size with the same direction of easy magnetization and does not possess a multiplicity of equally unsatisfied states such as frustration, it is not transformed into the spin glass at sufficiently low temperature. The ferromagnetic cluster exerts an influence on the neighbouring spin-glass state.

T_f depends on plastic strain as shown in figure 5. The spin-glass state is also influenced by the ferromagnetic clusters along the APB ribbon. T_f increases with the growth of the ferromagnetic clusters. On the other hand, T_f increases with increasing Fe content as shown in figure 2. The ferromagnetic cluster grows as the Fe content increases. The growth of ferromagnetic clusters increases T_f. The dependence of T_f on plastic strain is consistent with the dependence on Fe content. T_f depends generally on the concentration of the magnetic impurities in Au–Fe and Cu–Mn alloys: T_f increases with increasing concentration of magnetic impurities. The present results on T_f agree qualitatively well with the general concept.

The critical condition for the transition from paramagnetic to spin glass or ferromagnetic to spin glass is the existence of small ferromagnetic domains which behave superparamagnetically or ferromagnetically above T_f. The critical composition of the Fe–Al compounds is 29.7 at.% Al concentration (Shukla and Wortis 1980). Below the critical Al concentration, the small ferromagnetic groups with different directions of easy magnetization are unified into one ferromagnetic state, where Fe–Fe atom pairs in the β-site arrange in three $\langle 100 \rangle$ directions with the same probability.

A strong uniaxial anisotropy has been discovered in Fe–Al compounds deformed plastically. An advanced experiment is required to obtain the precise information on the induced anisotropy using a single crystal. A more detailed study is now in progress.

Acknowledgment

The authors express their thanks to Mr E Takahashi, Mr N Takahashi and Mr T Matsumoto for their help in the experiment and Dr W Sprengel for his reading of the manuscript.

References

Alloul H 1979 *J. Appl. Phys.* **50** 7330
Arrott A and Sato H 1959 *Phys. Rev.* **114** 1420
Besnus M, Herr A and Meyer A J 1975 *J. Phys. F: Met. Phys.* **5** 2138
Cable J W, David L and Parra R 1977 *Phys. Rev.* B**16** 1132
Chikazumi S, Suzuki K and Iwata H 1960 *J. Phys. Soc. Japan* **15** 250
Danan H and Gengnagel 1968 *J. Appl. Phys.* **39** 678
Huffman G P and Fisher R M 1967 *J. Appl. Phys.* **38** 735
Jakubovics J P, Lapworth A J and Jolly T W 1978 *J. Appl. Phys.* **49** 2002
Lapworth A J, Jakubovics J P and Baker G S 1971 *J. Physique Coll.* **32** C1 259
Néel L 1954 *J. Physique Radium* **15** 225
Okamoto H and Beck P A 1971 *Metall. Trans.* **2** 569
Parthasarathi A and Beck P A 1976 *Solid State Commun.* **18** 211
Sato H and Arrott A 1959 *Phys. Rev.* **114** 1427
Schultz S, Gullikson E M and Fredkin D R 1980 *Phys. Rev. Lett.* **45** 1508
Shukla P and Wortis M 1980 *Phys. Rev.* B**21** 159
Shull R D, Okamoto H and Beck P A 1976 *Solid State Commun.* **20** 863
Takahashi S 1972 *Phys. Status Solidi* b **52** 141
——1975 *Phys. Status Solidi* b **69** 227
——1986 *J. Magn. Magn. Mater.* **54–56** 1065
Takahashi S and Umakoshi Y 1990 *J. Phys.: Condens. Matter* **2** 4007
——1991 *J. Phys.: Condens. Matter* **3** 5805
Taniguchi S and Yamamoto M 1954 *Sci. Rep. Res. Inst. Tohoku Univ.* A **6** 336
Taylor A and Jones R M 1958 *J. Phys. Chem. Solids* **6** 16